



HAL
open science

Chlorination and bromination of 1,3-diphenylguanidine and 1,3-di-o-tolylguanidine: Kinetics, transformation products and toxicity assessment

Benigno J. Sieira, Rosa Montes, Arnaud Touffet, Rosario Rodil, Rafael Cela, Hervé Gallard, José Benito Quintana

► To cite this version:

Benigno J. Sieira, Rosa Montes, Arnaud Touffet, Rosario Rodil, Rafael Cela, et al.. Chlorination and bromination of 1,3-diphenylguanidine and 1,3-di-o-tolylguanidine: Kinetics, transformation products and toxicity assessment. *Journal of Hazardous Materials*, 2020, 385, pp.121590 -. 10.1016/j.jhazmat.2019.121590 . hal-03488734

HAL Id: hal-03488734

<https://hal.science/hal-03488734>

Submitted on 21 Jul 2022

HAL is a multi-disciplinary open access archive for the deposit and dissemination of scientific research documents, whether they are published or not. The documents may come from teaching and research institutions in France or abroad, or from public or private research centers.

L'archive ouverte pluridisciplinaire **HAL**, est destinée au dépôt et à la diffusion de documents scientifiques de niveau recherche, publiés ou non, émanant des établissements d'enseignement et de recherche français ou étrangers, des laboratoires publics ou privés.



Distributed under a Creative Commons Attribution - NonCommercial 4.0 International License

1 CHLORINATION AND BROMINATION OF 1,3-DIPHENYLGUANIDINE AND 1,3-DI-O-
2 TOLYLGUANIDINE: KINETICS, TRANSFORMATION PRODUCTS AND TOXICITY
3 ASSESSMENT

4 Benigno J. Sieira ¹, Rosa Montes ¹, Arnaud Touffet ², Rosario Rodil ¹, Rafael Cela ¹,
5 Hervé Gallard ^{2*}, José Benito Quintana ^{1*}

6 ¹ Department of Analytical Chemistry, Nutrition and Food Sciences, Institute of Food
7 Analysis and Research (IIAA), Universidade de Santiago de Compostela, R/ Constantino
8 Candeira S/N, 15782 – Santiago de Compostela (Spain)

9 ² Institute de Chimie des Milieux et des Matériaux de Poitiers (IC2MP), École Nationale
10 Supérieure d'Ingénieurs de Poitiers (ENSIP), Université de Poitiers, 1, rue Marcel Doré,
11 TSA 41105, 86073 – Poitiers (France)

12 * Corresponding authors:

13 Hervé Gallard: herve.gallard@univ-poitiers.fr

14 José Benito Quintana. jb.quintana@usc.es

15

16 **Abstract**

17 This work investigates the chlorination and bromination of two rubber and polymer
18 related chemicals, which have emerged as relevant water contaminants, i.e. 1,3-di-o-
19 tolylguanidine (DTG) and 1,3-diphenylguanidine (DPG). Kinetic constants at different
20 pH values were obtained and modelled, taking into account the pK_a values of DTG/DPG
21 and HClO, showing that the maximum reaction rate ($k_{app} > 10^4 \text{ M}^{-1} \text{ s}^{-1}$) is obtained at
22 pH values 8.8 for DPG and 9.1 for DTG. Bromination is also very fast, although unlike
23 chlorination, deviation from the model was observed at neutral pH, which was
24 attributed to formation of metastable transformation product (TP). A total of 35 TPs,
25 corresponding to halogenation, hydroxylation, formation of monophenylguanidine
26 derivatives and cyclization reactions, were tentatively identified. Furthermore it was
27 found that chloroform can be formed up to a 25% molar yield, while
28 dichloroacetonitrile was formed into less than a 3% yield. Several ecotoxicological
29 endpoints were predicted by quantitative structure–activity relationship models
30 (QSAR) for the TPs, some of which were predicted to be more toxic than DPG/DTG.
31 Also a chlorinated solution investigated by a *Vibrio Fisheri* acute toxicity test,
32 confirmed that toxicity increases with chlorination.

33 **Keywords**

34 Halogenation; transformation products; high-resolution mass spectrometry (HRMS);
35 ecotoxicity; disinfection by-products.

36 1. Introduction

37 Polar organic compounds, if persistent, spread along the water cycle, even becoming a
38 human health problem if that substances reach drinking waters (Hernández et al.
39 2015, Reemtsma et al. 2016, Schulze et al. 2019). 1,3-Di-*o*-tolylguanidine (DTG) and
40 1,3-diphenylguanidine (DPG) are chemicals used as accelerators in the vulcanization
41 processes of rubber and other polymers manufacture, with a registered production in
42 Europe, according to the REACH dossiers, in the 100-1000 tons (DTG) and 1000-10,000
43 tons (DPG) (ECHA 2018a, b). However, so far, little information about their
44 environmental (particularly water) occurrence is available. A first study from Montes et
45 al. (Montes et al. 2017), in the frame of the project PROMOTE (Metcalfé et al. 2003),
46 reported DTG occurring in environmental water samples across Europe by liquid
47 chromatography-high resolution mass spectrometry (LC-HRMS) screening. Later on,
48 within the same project, it has been shown that DPG as well as DTG occur in different
49 water compartments at the ng L⁻¹ level (Montes et al. 2019, Schulze et al. 2019). Zahn
50 et al. have recently shown that, when considering natural processes, DPG (DTG was
51 not considered in that study) photolyzes and reacts with manganese oxide, but does
52 not biodegrade and is stable to hydrolysis (Zahn et al. 2019). Furthermore, this
53 compound has been identified in drinking water in China at 0.7 mg L⁻¹, migrating from
54 polyethylene pipes (Tang et al. 2015) and, more recently, has also been recently
55 identified as being the major chemical leaching from tire wear particles (Hübner et al.
56 2019, Zahn et al. 2019). Furthermore, there is some literature that describes DTG and
57 DPG toxicity and pharmacological activity in mice and rats (Jaramillo-Ioranca and Es-
58 ram 2015, Lamy et al. 2010).

59 Yet, the possible reaction of both chemicals with chemical oxidants used in drinking
60 water treatment plants (DWTPs) and wastewater treatment plants (WWTPs) has not
61 been studied so far. Several disinfection techniques and processes are employed in
62 DWTPs and WWTPs. Among them, chlorine is the oxidant used in the vast majority of
63 DWTPs in Europe, and also in some WWTPs to a minor extent (Benitez et al. 2011,
64 Quintana et al. 2014). Although chlorine is effective to inactivate bacteria, the
65 formation of possible harmful transformation products (TPs), including well-known
66 disinfection byproducts (DBPs), as e.g. trihalomethanes, needs to be taken into
67 account (Acero et al. 2013, Postigo and Richardson 2014, Quintana et al. 2014, Rodil et
68 al. 2012). Such TPs (including DBPs) may in some cases be more (eco)toxic than the
69 precursor chemicals themselves (Postigo and Richardson 2014, Quintana et al. 2014).
70 Therefore, their identification is necessary in order to obtain a relevant interpretation
71 of the reaction.

72 Thus, the aim of this work was to perform a comprehensive study about the
73 chlorination of DTG and DPG in water. This includes a kinetic study and modelling,
74 identification of TPs (including those formed by bromination, since hypobromite is
75 rapidly formed from bromide into solution during chlorination (Benitez et al. 2011)) by
76 LC-HRMS, quantification of the yield of known DBPs formed and preliminary
77 (eco)toxicological assessment.

78

79 2. Materials and methods

80 2.1. Chemicals and stock solutions

81 DTG (99%) and DPG (97%) were purchased from Sigma-Aldrich (Steinheim, Germany)
82 and stock solutions were prepared in ultra-pure water. Ultra-pure water was obtained
83 directly in the lab from a Milli-Q Gradient A-10 system (Millipore, Bedford, MA, USA).
84 All solutions and dilutions necessary for the experiments were done in ultra-pure
85 water until desired concentration.

86 Sodium hypochlorite (8-14% Cl₂), ammonium chloride (> 99%) and potassium
87 phosphate dibasic trihydrate (> 99%) were obtained from Sigma-Aldrich. Sodium
88 thiosulfate (99.5%) and potassium bromide were from ACS Acros Organics (Thermo
89 Fisher Scientific, Waltham, MA, USA) and potassium di-hydrogen phosphate (99.5%)
90 was from Panreac (Barcelona, Spain). Standard solutions of chloroform and
91 haloacetonitriles (HANs) were prepared from EPA 551B Halogenated Volatiles Mix
92 supplied from Supelco. The exact nominal free chlorine content employed was
93 regularly determined spectrophotometrically by measuring the hypochlorite anion
94 absorption at 292 nm ($\epsilon = 350 \text{ L}^{-1} \text{ cm}^{-1}$) (Johnson and Melbourne 1996) of the stock
95 solution (pH >10).

96 2.2. Real samples

97 Two samples were used to study the extent of the chlorination reaction with a real
98 matrix. A surface water sample was collected from the River Sarela in Santiago de
99 Compostela (pH 6.8, Dissolved Organic Carbon: 2.42 mg L⁻¹, chloride: 7.98 mg L⁻¹,
100 bromide: 0.043 mg L⁻¹). A wastewater effluent was collected from a WWTP comprising
101 a primary and a secondary conventional sludge treatment (pH: 7.5, Dissolved Organic

102 Carbon: 14.1 mg L⁻¹, chloride: 23.1 mg L⁻¹, bromide: 0.075 mg L⁻¹). Dissolved organic
103 carbon was measured with a Shimadzu 5000A TOC analyzer (Duisburg, Germany),
104 while bromide and chloride were determined with a Metrohm 850 Professional Ion
105 Chromatograph (Zofingen, Switzerland).

106 **2.3. Chlorination experiments**

107 Chlorination of DTG and DPG were performed individually in 100 mL amber closed vials
108 at room temperature. Also, experiments without chlorine were prepared as a control.

109 Experiments to study chlorination kinetics were performed in a similar way, but with
110 lower compound concentrations (1 μM), an excess of chlorine (10 μM, 20 μM or 50
111 μM) and different pH of sample (5-12) being considered in 10 mM phosphate buffer
112 and NaOH for very basic pHs. Aliquots of 1 mL were taken at different reaction times
113 and the reaction stopped with 20 μL of 0.01 M sodium thiosulfate before residual
114 concentration of guanidine was analysed by liquid chromatography-photodiode array
115 detection (LC-PDA). Ammonium chloride (1 mM) was used in some experiments as
116 “soft” quenching method as being selective to free chlorine and as to avoid any
117 Na₂S₂O₃-induced back reaction that could interfere with determination of rate
118 constant (Dodd and Huang 2004). An experiment was also performed without stopping
119 the reaction and aliquots were manually injected at different reaction times using a
120 Rheodyne valve in the LC-PDA system.

121 Experiments were performed at room temperature (22 ±1°C). The pH was measured
122 before and after the experiment, and variation was less than 0.1 unit. Free active
123 chlorine was analysed by DPD colorimetric method (Clesceri et al. 1998) at the end of

124 reaction time. Chlorine consumption was usually below 10% and pseudo-first-order
125 plots were always linear (see Figure S1 for examples).

126 Additional experiments for the identification of TPs (performed in triplicate) were
127 carried out with a similar procedure. For these experiments, ultrapure water adjusted
128 at pH 7.0 was used, spiked with the compound at 10 μM , and initial chlorine dose set
129 to 100 μM . TPs were identified after reduction by ascorbic acid for reaction times of 30
130 s, 1 min, 2 min, 5 min, 10 min and 30 min.

131 DBPs formation potentials (chloroform and haloacetonitriles) were determined for a
132 reaction time of 2 days at pH 7.0 in ultrapure water with an initial concentration (of
133 either DPG or DTG) of 10 μM and molar chlorine to guanidine ratios of 1, 10 and 100 in
134 headspace-free conditions.

135 **2.4. Bromination experiments**

136 Bromination experiments were performed under the same conditions as chlorination,
137 in order to determine apparent rate constants and detect TPs that can be produced in
138 bromide containing waters. Bromine was generated in the lab according to the
139 procedure described by Benitez et al. (Benitez et al. 2011). Briefly, bromine was
140 produced from the reaction between 9 mM HOCl and 10 mM potassium bromide. The
141 yield of this reaction was followed spectrophotometrically (hypobromite anion
142 maximum absorption wavelength at 329 nm with an $\epsilon = 332 \text{ M}^{-1} \text{ cm}^{-1}$ at pH above 11.5)
143 (Benitez et al. 2011).

144 Kinetics of bromination were studied as for chlorination for pH values ranging from 5
145 to 9 using direct method in batch reactor with an excess of bromine (10 to 100 μM)
146 compared to 1 μM DPG or DTG solution (see Figure S2 for examples of bromination of

147 DPG). Apparent rate constants were also determined by using the competition kinetics
148 method (Acero et al., 2005) with 4-bromophenol (BP) in pH 8 - 11 range or 2,4,6-
149 tribromophenol (TBP) at pH 7.0 and 8.0 as reference compounds (see Figure S3). In this
150 method, different concentrations of bromine from 0 to 10 μM were introduced in 25
151 mL of a 10 mM phosphate buffer solution containing 5 μM DPG or DTG and 5 μM
152 reference compound (either BP or TBP). Residual concentrations of organic
153 compounds were determined by LC-PDA. Apparent rate constants of BP and TBP were
154 calculated for each pH from intrinsic rate constants compiled by Heeb et al. (2014) and
155 $\text{pK}_a_{\text{HOBr/BrO}^-} = 8.8$. Values are given in Table S3 and S4. An apparent rate constant of
156 $2063 \text{ M}^{-1} \text{ s}^{-1}$ was determined for the reaction of bromine with TBP at pH 6.94 by direct
157 method using 20 μM bromine and 1 μM TBP (Figure S4); value similar to $2100 \text{ M}^{-1} \text{ s}^{-1}$
158 determined by Acero et al. (2005) and used in this study.

159 **2.5. Liquid chromatography - photodiode array detection (LC-PDA)**

160 The chlorination kinetic study was followed by analysing the samples in a LC-PDA
161 system. The instrument was a Waters 2695 LC (Milford, MA, USA) equipped with a
162 degasser, binary high-pressure pump, LC column oven and an autosampler. The PDA
163 was a Waters 2996 equipped with a deuterium lamp. DPG was monitored at 235 nm,
164 whereas DTG, BP and TBP were measured at 225 nm.

165 The LC column used was a 250 mm x 4.6 mm; 5 μm Kinetex EVO C18 (Phenomenex,
166 Torrance, CA, USA) at a flow rate of 1 mL min^{-1} . Mobile phase consisted in Milli-Q
167 water (eluent A) and acetonitrile (eluent B), both acidified with 0.1 % formic acid.
168 Gradient was as follows: 0 min, 5% B; 10 min, 100% B; 12 min, 100% B; 12.10 min, 5%

169 B; 20 min, 5% B. Injection volume was set to 50 μ L. Instrument control and data
170 treatment were done with Empower software (Waters).

171 **2.6. LC-HRMS**

172 The system used for the determination of TPs was an Agilent 1200 Series LC (Agilent
173 Technologies, Santa Clara, CA, USA) equipped with a degasser, a binary high-pressure
174 pump, LC column oven and an autosampler. This LC system was interfaced to an
175 Agilent 6520 Series Quadrupole-Time of Flight (QTOF) MS equipped with a Dual
176 Electrospray (Dual-ESI) ion source.

177 The LC column was a Luna 150 mm x 2 mm; 3 μ m C18 (2) (Phenomenex) at a flow of
178 mobile phase of 0.2 mL min⁻¹, and column temperature established at 35 °C. Mobile
179 phase and gradient used are the same as described in Section 2.5. Injection volume
180 was set at 10 μ L.

181 For the QTOF, Nitrogen (99.999%) used for nebulising and drying gas was supplied by a
182 nitrogen generator (Erre Due Srl, Livorno, Italy). Collision-Induced Dissociation (CID) in
183 tandem mass spectrometry analysis (MS/MS) was performed with Nitrogen
184 (99.9995%) purchased from Praxair (Santiago de Compostela, Spain) as collision gas.
185 ESI source operated in positive (no TPs were detected in negative) polarity and its
186 parameters were as follows: gas temperature 350 °C; drying gas 5 L min⁻¹; nebulizer 42
187 psig, capillary 4000 V; fragmentor 120 V; skimmer 65 V; and octapole RF 750 V.
188 Instrument acquired MS spectra in centroid mode and operated at 2 GHz (extended-
189 dynamic range), which provided a Full Width at Half Maximum (FWHM) resolution of
190 ca. 4500 at m/z 121 and ca. 11000 at m/z 922, scan range: 70-1000 m/z. The
191 manufacturer reference solution was also infused during every run and ionized with

192 the second sprayer of the Dual-ESI at 5 psig, to calibrate automatically and keep the
193 mass accuracy. In this solution, two masses, m/z 121.0509 and 922.0098 for ESI (+)
194 were used for m/z -axis continuous recalibration.

195 Instrument control and data treatment were done with different software included in
196 the MassHunter package (Agilent Technologies). Determination of TPs was performed
197 as described elsewhere (Carpinteiro et al. 2017). Briefly, the algorithm “Find by
198 Molecular Feature” from the MassHunter Qualitative (Agilent Technologies) software
199 was used to generate a list of features (chromatographic peaks and m/z values) with a
200 response higher than 1000 counts. Data obtained was then analysed with the software
201 Mass Profiler Professional (Agilent Technologies) that compares the intensity of those
202 features at different reaction times, where features whose intensity increases as
203 compared to time 0 can be possible TPs. Then, formulas were generated for those
204 features. The isotope pattern matching as well as error between the experimental m/z
205 values and those calculated (from the generated formula) is grouped by the software
206 to provide a score in percentage, in which 100% would indicate a perfect match.

207 Tandem mass spectrometry (MS/MS) analysis were obtained for the structure
208 elucidation of the TPs structures, using CID with different collision energies between
209 10 and 40 V.

210 **2.7. Determination of DBPs**

211 Chloroform was analysed by headspace injection and gas chromatography coupled to
212 mass spectrometry detection (GC-MS). Analysis was performed by using a CTC
213 Analytics Combi Pal autosampler with an Agilent 7890 GC and an Agilent 5975C mass
214 spectrometer. 10 mL of sample were poured in 20 mL headspace vials containing 10 μ L

215 of 1M ascorbic acid to quench residual chlorine. Vials were heated at 50°C and stirred
216 at 500 rpm for 10 min before 2.5 mL gas phase was injected into the gas
217 chromatography in pulsed split mode (ratio 1:10). The analytical column was an Agilent
218 HP-5MS column (30 m x 0.25 mm; film thickness 1 µm). Retention time of chloroform
219 was 3.8 min for temperature program starting at 40°C and ending at 55°C in 8 min.

220 Haloacetonitriles (HANs) were analysed by the 551.1 EPA extraction method followed
221 by GC-MS determination as described elsewhere (Le Roux et al. 2011). Detection limits
222 for DBPs were 0.1 µg L⁻¹.

223 **2.8. Toxicity assessment**

224 An estimation of the (eco)toxicity was done for DTG, DPG and the identified TPs by
225 using the US Environmental Protection Agency Toxicity Estimation Software Tool
226 (TEST) version 4.1, which provides a prediction of the toxicity according to
227 quantitative-structure property relationships (QSAR) by the consensus method, which
228 uses an average value of the calculated toxicities by five different developed QSAR
229 methodologies (Carpinteiro et al. 2017, González-Mariño et al. 2015). Only the oral rat
230 LC₅₀, *Daphnia Magna* LC₅₀ and *Tetrahymena pyriformis* 50% growth inhibition
231 concentration (IGC₅₀) were considered since other ecotoxicological endpoints could
232 not be calculated by the software for most TPs.

233 Besides the QSAR prediction, a bioluminescent *Vibrio Fisheri* test evaluation of the
234 toxicity of DPG and DTG and different chlorination mixtures was performed according
235 to the standard method NF EN ISO 11348-3 (2009) by using a LumisTox® 300. Details of
236 the procedure are described elsewhere (Tawk et al. 2015).

237

238 3. Results and Discussion

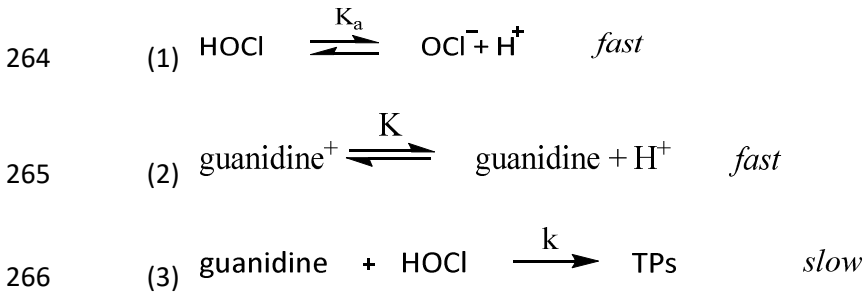
239 3.1. Chlorination kinetic study

240 A full kinetic study of DTG and DPG reaction with chlorine was performed considering a
241 wide range of pH from 5 to 11-12. In excess of chlorine, results were adjusted to a
242 pseudo-first order kinetic equation (Figure S1a) to obtain the observed rate constant
243 k_{obs} in s^{-1} as the slope of the linear regression. The first order with respect to chlorine
244 was verified by changing the initial concentration of chlorine (Figure S1b). In addition,
245 it was verified that guanidine concentrations were similar when thiosulfate or
246 ammonium chloride were used to stop the reaction or when manual injection was
247 used without quenching the reaction (Figure S1a) suggesting that N-chlorinated
248 guanidine was not formed (Dodd and Huang 2004).

249 The apparent rate constant (k_{app} in $M^{-1} s^{-1}$) was determined for each experiment from
250 k_{obs} value and the initial concentration of chlorine. The values of k_{app} are compiled in
251 Tables S1 and S2. They range from $32 M^{-1} s^{-1}$ at pH 5 to a maximum of ca. $1.11 \times 10^4 M^{-1}$
252 s^{-1} at pH 8.4 for DPG. In the case of DTG, reaction is even faster, with k_{app} ranging
253 from 25 (at pH 4.9, the lowest pH tested in this case) to $1.83 \times 10^4 M^{-1} s^{-1}$ at pH 9.9. At
254 natural water pH values, this translates in very fast reactions, with half-lives of a few
255 seconds to some minutes with typical chlorine doses ($1-10 mg L^{-1}$).

256 A theoretical model of the pH-dependent apparent rate constant (k_{app}) for the reaction
257 between each guanidine and chlorine was described based on the speciation of
258 HOCl/CIO⁻ ($pK_a = 7.54$) and guanidines ($pK_a = 10.67$ for DTG, and $pK_a = 10.12$ for DPG
259 (Perrin 1965)) and considering HOCl as the only active electrophile (Gallard and von
260 Gunten 2002). The large increase in k_{app} when the pH increased from 5 to 9 suggests a

261 greater contribution of the neutral guanidine to the protonated form. Thus, the
 262 resulting model for the DTG and DPG reaction mechanism is described as follows
 263 assuming that HOCl reacts only with neutral guanidine species in the first assumption:



267 The general expression for the reaction of the guanidine compound (either DPG or
 268 DTG) with chlorine is then:

269 (4) $\frac{d[\text{guanidine}]_T}{dt} = -k[\text{guanidine}][\text{HOCl}] = -k_{app}[\text{guanidine}]_T[\text{HOCl}]_T$ and

270 (5) $k_{app} = k \alpha_{\text{HOCl}} \alpha_{\text{guanidine}}$

271 where: k is the specific rate constant of HOCl with the neutral species of DTG/DPG,
 272 K_a is the acid-base equilibrium constant of HOCl, $[\text{HOCl}]_T$ is the total concentration of
 273 free chlorine ($\text{HOCl} + \text{OCl}^-$), $[\text{guanidine}]_T$ is the total concentration of DPG or DTG, and
 274 α_{HOCl} and $\alpha_{\text{guanidine}}$ are the molar fractions of HOCl and neutral guanidine species,
 275 respectively.

276 By introducing the expression of both, HOCl and guanidine molar fractions, the k_{app}
 277 value is given by the following expression:

278 (6) $k_{app} = \frac{k K [H^+]}{(K + [H^+])(K_a + [H^+])}$

279 The value of the rate constant k was determined by a non-linear least-square
280 regression of the experimental pH profile of the k_{app} values using Sigma Plot 11.0
281 (Systat Software Inc., San Jose, CA, USA).

282 The pH dependence of k_{app} is shown in Figures 1a and 1b for DPG and DTG,
283 respectively. For both compounds, the pH profile exhibits a maximum between pH 8
284 and pH 10. This maximum corresponds to the concomitant presence of both HOCl and
285 neutral guanidine. The maximum pH value is equal to the average value of the pK_a of
286 HOCl and guanidines i.e. 8.8 for DPG and 9.1 for DTG. As shown in Figure 1, the model
287 fits well with the experimental data considering only the reaction of HOCl with neutral
288 guanidine. No improvement was obtained by including the reaction of ClO^- with
289 neutral guanidine and the reaction of HOCl with protonated guanidine (see Text S1 and
290 Table S5), which is in accordance with the literature (Deborde and von Gunten 2002).
291 The rate constants, k , of the reactions between HOCl and DPG and DTG neutral species
292 determined from model fitting to the experimental values are $4.1 (\pm 0.3) \times 10^6 \text{ M}^{-1} \text{ s}^{-1}$
293 and $2.6 (\pm 0.1) \times 10^7 \text{ M}^{-1} \text{ s}^{-1}$ for DPG and DTG, respectively. The apparent rate constants
294 at neutral pH ($\sim 10^3 \text{ M}^{-1} \text{ s}^{-1}$) and intrinsic rate constants (k) of neutral species ($\sim 10^6 - 10^7$
295 $\text{M}^{-1} \text{ s}^{-1}$) are in the range of rate constants of secondary amines with chlorine (Deborde
296 and von Gunten 2008). However, N-chloroamino compounds were not detected during
297 kinetic experiments and identification of TPs would indicate that initial reactive site is
298 the aromatic ring. Lower rate constant of $19 \text{ M}^{-1} \text{ s}^{-1}$ was obtained for ethyl guanidine at
299 pH 7.2 – 7.4 (Pattison and Davies 2001), which can be explained by the stronger basic
300 character of alkyl guanidines.

301 **3.2. Bromination kinetic study**

302 The apparent rate constants of bromination determined by using direct and
303 competition kinetics methods are listed in Table S3 and S4 for DPG and DTG,
304 respectively and are plotted versus pH in Figure 2. Examples of pseudo-first-order and
305 competition kinetics plots are given in Figure S2 and Figure S3 for DPG. The apparent
306 rate constants range from 76 to $2.89 \times 10^5 \text{ M}^{-1} \text{ s}^{-1}$ for DPG and from 36 to $5.87 \times 10^4 \text{ M}^{-1}$
307 s^{-1} for DTG. In contrast to chlorine, lower rate constants were determined for DTG,
308 which could be attributed to steric effects between the bulky bromine atoms and the
309 methyl groups in DTG.

310 The experimental results fit well with the proposed model at pHs below 6 and above 9,
311 while a strong deviation and even discrepancies between rate constants determined
312 by the direct kinetics method and the competition kinetics method using BP as
313 reference compound in the pH 7 – 9 range. Such deviations are attributed to a
314 metastable TP with oxidizing properties which could not be identified by LC-HRMS in
315 that pH range (see detailed discussion in Text S2 and Figures S3-S6).

316 Excluding those pH values, and compared to chlorination, maximum k_{app} values are
317 slightly shifted to higher pH values due to the higher pK_a of HOBr ($\text{pK}_a = 8.8$).
318 Calculated intrinsic rate constants for the reaction of HOBr with neutral DPG and DTG
319 were $8.3 (\pm 0.4) \times 10^6$ and $5.5 (\pm 0.7) \times 10^6$, respectively. While HOBr reacts usually much
320 faster than HOCl with organic compounds (Heeb et al., 2014), the rate constant of
321 HOBr with DPG was only twice as high as the reaction of HOCl with DPG and the rate
322 constant for the reaction of HOBr with DTG was lower than that of HOCl. Steric
323 hindrance (as mentioned), different reactive sites and type of reaction (oxidation vs

324 substitution) might explain this unexpected result, which requires further
325 investigation.

326 **3.3. Transformation products**

327 Identification of TPs was performed for both DTP and DPG considering chlorination
328 and bromination. Experiments were carried out as described in sections 2.3 and 2.4. All
329 samples were analysed in the LC-QTOF equipment as detailed in 2.6. The proposed
330 structures of the TPs are presented in Figures 3 and 4. Further details on formulas,
331 mass errors and scores of the TPs, as well as individual structures derived from the
332 interpretation of MS/MS spectra are presented in Tables S6 and S7. TPs were named
333 with the precursor compound abbreviation followed by the nominal mass of its $[M+H]^+$
334 ion. As it can be observed the empirical formula could be proposed with a high degree
335 of certainty, with score values higher than 95% and mass errors lower than 5 ppm,
336 except for DTG-274, whose score was 79% and mass error was 9.7 ppm due to its low
337 intensity.

338 The proposed structures are based on the interpretation of the MS/MS spectra, which
339 are presented into Figures S7 and S8, for DPG and DTG TPs, respectively. Moreover,
340 DPG-136 (i.e. monophenylguanidine) was unequivocally identified by purchasing its
341 authentic standard from Sigma-Aldrich.

342 There are four main types of reactions occurring during chlorination, i.e. ipso-
343 chlorination to produce monoguanidine derivatives, introduction of chlorine atoms
344 (bromine when samples are brominated) into an aromatic ring, hydroxylation and
345 intramolecular cyclization. Thus, DPG-136 was easily identified by its spectrum (Figure
346 S7), and because an authentic standard was available, as mentioned. This TP further

347 reacts by halogenation to the corresponding chlorinated or brominated derivatives
348 (DPG-170 and DPG-214), easily identified because their MS/MS spectra is similar to
349 DPG-136 and exhibit the halogen isotopic pattern (Figure S7). DPG-119 is also
350 produced at long reaction times. Hydroxylation of DPG produces DPG-228, while
351 halogenation produces DPG-246 (chlorination) and DPG-290 (bromination), all of them
352 easily identified by their MS/MS spectra (Figure S7).

353 A key TP is DPG-210, which a similar empirical formula than DPG itself but with one
354 further double-bond equivalent (i.e. 2 atoms of H less), Table S6. Its MS/MS spectrum
355 exhibits first the loss of ammonia to m/z 192.0671 and also the elimination of CH_3N_2 to
356 m/z 167.0720 from the protonated molecular ion (Figure S7e). This second ion would
357 not be possible unless a cycle is formed. Because of this, we hypothesize here that
358 DPG-210 corresponds to the structure shown in Figure 3, by formation of the 7-
359 membering cycle from DPG-228 (hydroxylated DPG) by elimination of water. In fact the
360 maximum intensity of DPG-228 was observed at 0.5 min and then its intensity rapidly
361 drops, while DPG-210 maximum is reached at 1 min and then drops more slowly (see
362 Figure S9a). The fact that DPG-210 has also been observed as a photolysis TP by Zahn
363 et al. (Zahn et al. 2019), although no structure was proposed in that publication,
364 further supports this hypothesis. Once DPG-210 is formed, this molecule further reacts
365 to yield a mono-hydroxylated-TP (DPG-226), a hydroxychloro-TP (DPG-260) or a
366 dichloro,hydroxy-TP (DPG-294).

367 In the case of DTG, the reaction was similar to DPG, as expected, but a larger number
368 of TPs could be identified (23 vs. 11 TPs). In general, the main difference in the TPs
369 produced is that a greater degree of hydroxylation and halogenation is observed, e.g.

370 DTG-308 (a dichlorinated derivative of DTG), which can be explained by the electron-
371 donor effect of the methyl group on aromatic ring. Although no MS/MS spectra (Figure
372 S8) was obtained for all TPs, due to the low intensity of some of them, structures
373 compiled into Figure 4 and Table S7 (those TPs without MS/MS data are marked with a
374 * symbol in the Table) were assigned on the basis of the MS/MS spectra (when
375 available) and by analogy to DPG TPs.

376 As regards of the most relevant TPs, Figures S9b and 10b present the normalized
377 amount of each TP and their precursors for a reaction with 100 μ M chlorine and up to
378 30 min of contact time. Normalization was performed by using the signal of the
379 original compound (DPG or DTG) as a surrogate to calculate an approximate yield,
380 except for DPG-136, DPG-119, DPG-170, DTG-150, DTG-166, DTG-184 and DTG-228,
381 where monophenyl-guanidine (DPG-136) was used instead, as being considered
382 structurally closer. In the case of DPG (Figure S9), the most intense TP is DPG-136 with
383 a yield of ca. 5% at 0.5-2 min, dropping down to 3% at 30 min. The second most
384 relevant TP is DPG-246 (monochloro-DPG), with a yield of ca. 3% at 0.5-2 min, dropping
385 down to ca. 0.2% at 30 min. It is noteworthy that at 30 min, there was no DPG
386 detectable and the sum of all TPs intensities would approximately represent a 5%
387 yield. This could likely be attributed to the formation of ring-opening products like
388 chloroform with a relatively high yield (see 3.4) and the uncertainty of the semi-
389 quantitative approach, due to the lack of authentic standards for most TPs.

390 In the case of DTG (Figure S10), the most intense TP is DTG-254 (hydroxylated cyclic
391 product) with a yield of ca. 30% at 0.5-2 min, followed by DTG-290 (hydroxy,chloro-
392 DTG) with a yield of ca. 15% at 0.5-2 min. These two TPs are also the most relevant at

393 30 min, representing an estimated yield of 4 and 8% respectively. Also, in the case of
394 DTG, the total yield of TPs at 30 min is ca. 20%.

395 **3.4. Disinfection by-products**

396 Subsequently to TPs identification, we investigated the formation potential of classical
397 DBPs (chloroform and HANs). Chloroform was measured as the only trihalomethane
398 that can be formed without bromide and representing the most relevant group of
399 DBPs, while HANs is another important group of DBPs which can be produced from N-
400 containing chemicals, as it is the case of DPG and DTG. Figure S11 shows the molar
401 yields of CHCl_3 and dichloroacetonitrile (DCAN), the only HAN detected, produced from
402 the chlorination of DPG and DTG after 2 day reaction time. Similar yields were
403 obtained for both guanidines. For CHCl_3 , the yield of ca. 25% for a molar guanidine/ Cl_2
404 ratio of 1:100 is similar to CHCl_3 yields ranging from 10 to 32% already described for
405 hydroxylated and chlorinated aromatic compounds (Gallard and von Gunten 2002).
406 This is consistent with the formation of chloro or/and hydroxy DPG and DTG that
407 further react with chlorine leading to CHCl_3 as end-product after ring cleavage. Among
408 HANs, only DCAN was detected at significant levels and with yields much lower than
409 CHCl_3 . For a ratio of 1:100, molar yields were 4.4% and 2.3% for DPG and DTG,
410 respectively.

411 **3.5. Reaction in real sample matrices**

412 The reactivity of both guanidine compounds was tested by spiking two real matrices (a
413 surface water and a wastewater effluent) with 1 μM (i.e., ca. 200 $\mu\text{g L}^{-1}$) of either DPG
414 or DTG and 10 μM chlorine and the reaction kinetics followed for 20 min (reaction
415 quenched with ascorbic acid) by LC-HRMS.

416 In the case of the surface water, DPG and DTG reacted rapidly, being below 1% of their
417 initial concentration after 2 min (Figure S12a-b). Conversely, with the effluent
418 wastewater (with a higher TOC), still an 87% of DPG and 73% of DTG remained after 20
419 min (Figure S12c-d). Indeed, formation of TPs is easier to happen during drinking water
420 production than by chlorination of wastewater (after secondary treatment). Even so,
421 the chlorinated wastewater was analysed for the TPs previously identified in ultrapure
422 water and several of them could be detected. The amount of bromide in those samples
423 is very low ($<0.1 \text{ mg L}^{-1}$, see 2.2), therefore no brominated TPs were detected. When
424 excluding those brominated TPs, 6 out of 9 TPs were detected for DPG (DPG-136,
425 DPG-228, DPG-210, DPG-226, DPG-260 and DPG-294) and 7 out 16 were detected for
426 DTG (DTG-150, DTG-256, DTG-290, DTG-239, DTG-254, DTG-270 and DTG-288).

427 **3.6. (Eco)toxicity assessment**

428 To obtain a preliminary estimation of the ecotoxicological implications of the
429 chlorination reaction, the US-EPA TEST software was used in order to predict the
430 toxicity of the two guanidines and their TPs. This prediction was performed only for
431 *Daphnia Magna* LC_{50} (48 h), *Tetrahymena Pyriformis* LC_{50} (48 h) and oral rat LD_{50} (as a
432 proxy of human toxicity), since the software was unable to produce an estimation for
433 other endpoints. The results obtained are summarized in Tables 1 and 2.

434 As it can be appreciated, oral rat toxicity LD_{50} values are in the $602\text{-}805 \text{ mg Kg}^{-1} \text{ bw}$ for
435 the two guanidines, which would classify them as Category 4 (i.e. the less toxic
436 category) according to the ECHA Guidance (ECHA 2017). The TPs would also be
437 classified as Category 4. Hence human toxicological hazard is expected to be low.

438 The predicted acute aquatic toxicity endpoint values lie in the 5-28 mg L⁻¹ and 3-6 mg L⁻¹
439 ranges, for DPG and DTG respectively (Tables 1 and 2). Thus, they would not be
440 classified as Category Acute 1 (the only acute aquatic toxicity category) according to
441 the ECHA Guidance (ECHA 2017). As regards the TPs, the predicted aquatic toxicity of
442 the monoguanidine TPs is lower than the precursor guanidines for the crustacean
443 *Daphnia Magna*, while it could not be predicted for the fish *T. pyriformis*. On the other
444 hand, particularly TPs which are halogenated are predicted to be more toxic. Thus,
445 DPG-294 and 14 TPs from DTG (see Table 1 and 2) would have a predicted toxicity
446 endpoint <1 mg L⁻¹ and would thus be classified in the Category Acute 1 for aquatic
447 organisms. Care must be taken with these data, since the third trophic level (algae)
448 toxicity could not be predicted and values obtained for algae can likely result into more
449 ecotoxicity. In fact DTG is classified in the REACH dossier as Aquatic Acute 1 (ECHA
450 2018a).

451 Furthermore, the acute toxicity of DPG and DTG was assessed using the
452 bioluminescent *Vibrio fischeri* test.

453 The EC₅₀ and EC₂₀ values of *Vibrio fischeri* test were estimated from a series of
454 geometrical dilutions with dilution factors from 1 to 256 and initial guanidine
455 concentration of 100 mg L⁻¹. Figure S13 shows two dose-response curves of DPG after
456 an incubation time of 30 min at 15°C. The initial EC₂₀ of DPG was 40 ±2 mg L⁻¹ and the
457 EC₅₀ was estimated (as detailed in Text S3) to be 245 ±33 mg L⁻¹ from extrapolation of
458 the dose-response curves. The toxicity of DTG was lower and only an EC₂₀ of 80 mg L⁻¹
459 could be determined. These results confirm that both guanidines have a low acute
460 aquatic toxicity. Due to solubility limitations, the effect of chlorination on acute toxicity

461 was only tested with a DPG solution of 40 mg L⁻¹ corresponding to the EC₂₀.
462 Chlorination was performed with chlorine doses of 40 and 400 mg Cl₂ L⁻¹ (i.e. molar
463 Cl₂/DPG ratio of 3 and 30). Toxicity tests were conducted after the absence of chlorine
464 residual was checked. Results in Figure 5 shows that the bioluminescence inhibition
465 strongly increases from 14% before chlorination to 45 and 99% for Cl₂/DPG ratios of 3
466 and 30, respectively. Similar results were generally observed in the literature after
467 chlorination and were assigned to more toxic halogenated TPs (El Najjar et al. 2013,
468 Tawk et al. 2015). Even though the increase of toxicity could not be assigned to specific
469 TPs/DBPs, results of bioluminescent *Vibrio fischeri* test were in agreement with
470 predicted aquatic toxicity endpoints obtained by QSAR.

471

472 **4. Conclusions**

473 DPG and DTG rapidly react with chlorine and bromine at natural water pH values. This
474 reaction leads to the formation of several TPs via ipso-halogenation, hydroxylation,
475 halogenation and cyclization. Several of these TPs are predicted to be more toxic than
476 the original guanidine compounds, which was confirmed by measuring the acute
477 toxicity of a chlorinated mixture by a *Vibrio Fisheri* acute toxicity assay. Moreover,
478 chlorination leads to the production of the traditional/regulated DBPs chloroform and,
479 to a minor extent, dichloroacetonitrile, when the molar ratio of chlorine to DPG/DTG is
480 high.

481

482 **Acknowledgements**

483 This work was supported by the Water Challenges for a Changing World Joint Program
484 Initiative (Water JPI) Pilot Call (ref. WATERJPI2013 – PROMOTE), funded by the Spanish
485 Ministry of Economy and Competitiveness/Spanish Agencia Estatal de Investigación
486 (refs. JPIW2013-117 and CTM2017-84763-C3-2-R) and French Office National de l'Eau
487 et des Milieux Aquatiques (ref. PROMOTE). We also acknowledge the Galician Council
488 of Culture, Education and Universities (ref. ED431C2017/36), Région Nouvelle
489 Aquitaine and FEDER/EDRF funding.

490 **REFERENCES**

491 Acero, J.L., Benitez, F.J., Real, F.J., Roldan, G. and Rodriguez, E. (2013) Chlorination and
492 bromination kinetics of emerging contaminants in aqueous systems. Chemical
493 Engineering Journal 219, 43-50.

494 Benitez, F.J., Acero, J.L., Real, F.J., Roldan, G. and Casas, F. (2011) Bromination of
495 selected pharmaceuticals in water matrices. Chemosphere 85(9), 1430-1437.

496 Carpinteiro, I., Rodil, R., Quintana, J.B. and Cela, R. (2017) Reaction of diazepam and
497 related benzodiazepines with chlorine. Kinetics, transformation products and in-silico
498 toxicological assessment. Water Research 120, 280-289.

499 Clesceri, L.S., Greenberg, A.E. and Eaton, A.D. (eds) (1998) Standard Methods for the
500 Examination of Water and Wastewater, American Water Works Association, Baltimore,
501 MD.

502 Deborde, M. and von Gunten, U. (2008) Reactions of chlorine with inorganic and
503 organic compounds during water treatment - Kinetics and mechanisms: A critical
504 review. Water Research 42(1-2), 13-51.

505 Dodd, M.C. and Huang, C.H. (2004) Transformation of the antibacterial agent
506 sulfamethoxazole in reactions with chlorine: Kinetics, mechanisms, and pathways.
507 Environmental Science and Technology 38(21), 5607-5615.

508 ECHA (2017) Guidance on the Application of the CLP Criteria. Guidance to Regulation
509 (EC) No 1272/2008 on classification, labelling and packaging (CLP) of substances and
510 mixtures. Version 5.0. July 2017. Agency, E.C. (ed), European Chemicals Agency,
511 Helsinki, Finland.

512 ECHA (2018a) 1,3-di-o-tolylguanidine (EC number: 202-577-6 | CAS number: 97-39-2)
513 REACH dossier, European Chemicals Agency.

514 ECHA (2018b) 1,3-diphenylguanidine (EC number: 203-002-1 | CAS number: 102-06-7)
515 REACH dossier, European Chemicals Agency.

516 El Najjar, N.H., Deborde, M., Journal, R. and Vel Leitner, N.K. (2013) Aqueous
517 chlorination of levofloxacin: Kinetic and mechanistic study, transformation product
518 identification and toxicity. *Water Research* 47(1), 121-129.

519 Gallard, H. and von Gunten, U. (2002) Chlorination of Phenols: Kinetics and Formation
520 of Chloroform. *Environmental Science & Technology* 36(5), 884-890.

521 González-Mariño, I., Quintana, J.B., Rodríguez, I., Cores, M. and Cela, R. (2015)
522 Transformation of methadone and its main human metabolite, 2-ethylidene-1,5-
523 dimethyl-3,3-diphenylpyrrolidine (EDDP), during water chlorination. *Water Research*
524 68, 759-770.

525 Hernández, F., Ibá, M., Portolés, T., Cervera, M.I., Sancho, J.V. and López, F.J. (2015)
526 Advancing towards universal screening for organic pollutants in waters. Journal of
527 Hazardous Materials 282, 86-95.

528 Hübner, D., Zahn, D., Huppertsberg, S. and Knepper, T.P. (2019) Tires and tire wear
529 particles as source of 1,3-diphenylguanidine and other organic micropollutants in the
530 aquatic environment, Erfurt (Germany).

531 Jaramillo-loranca, B.E. and Es-ram, L.G. (2015) The Sigma Agonist 1 , 3-Di- o -tolyl-
532 guanidine Reduces the Morphological and Behavioral Changes Induced by Neonatal
533 Ventral Hippocampus Lesion in Rats. Synapse 225(February), 213-225.

534 Johnson, M. and Melbourne, P. (1996) Photolytic spectroscopic quantification of
535 residual chlorine in potable waters. Analyst 121(8), 1075-1078.

536 Lamy, C., Scuvée-Moreau, J., Dilly, S., Liégeois, J.F. and Seutin, V. (2010) The sigma
537 agonist 1,3-di-o-tolyl-guanidine directly blocks SK channels in dopaminergic neurons
538 and in cell lines. European Journal of Pharmacology 641(1), 23-28.

539 Le Roux, J., Gallard, H. and Croué, J.-P. (2011) Chloramination of nitrogenous
540 contaminants (pharmaceuticals and pesticides): NDMA and halogenated DBPs
541 formation. Water Research 45(10), 3164-3174.

542 Metcalfe, C.D., Miao, X.S., Koenig, B.G. and Struger, J. (2003) Distribution of acidic and
543 neutral drugs in surface waters near sewage treatment plants in the lower Great Lakes,
544 Canada. *Environmental Toxicology And Chemistry* 22(12), 2881-2889.

545 Montes, R., Aguirre, J., Vidal, X., Rodil, R., Cela, R. and Quintana, J.B. (2017) Screening
546 for Polar Chemicals in Water by Trifunctional Mixed-Mode Liquid Chromatography–
547 High Resolution Mass Spectrometry. *Environmental Science & Technology* 51(11),
548 6250-6259.

549 Montes, R., Rodil, R., Cela, R. and Quintana, J.B. (2019) Determination of persistent and
550 mobile organic contaminants (PMOCs) in water samples by mixed-mode liquid
551 chromatography-tandem mass spectrometry. *Analytical Chemistry* 91(8), 5176-5183.

552 Pattison, D.I. and Davies, M.J. (2001) Absolute Rate Constants for the Reaction of
553 Hypochlorous Acid with Protein Side Chains and Peptide Bonds. *Chemical Research in*
554 *Toxicology* 14(10), 1453-1464.

555 Perrin, D.D. (1965) Dissociation constants of organic bases in aqueous solution, IUPAC
556 Publications, London, Butterworths.

557 Postigo, C. and Richardson, S.D. (2014) Transformation of pharmaceuticals during
558 oxidation/disinfection processes in drinking water treatment. *Journal of Hazardous*
559 *Materials* 279, 461-475.

560 Quintana, J.B., Rodil, R. and Rodríguez, I. (2014) Transformation Products of Emerging
561 Contaminants in the Environment. IN: Lambropoulou, D.A. and Nollet, L.M.L. (eds), pp.
562 123-160, John Wiley and Sons Ltd.

563 Reemtsma, T., Berger, U., Arp, H.P.H., Gallard, H., Knepper, T.P., Neumann, M.,
564 Quintana, J.B. and Voogt, P.D. (2016) Mind the Gap: Persistent and Mobile Organic
565 Compounds - Water Contaminants That Slip Through. Environmental Science &
566 Technology 50(19), 10308-10315.

567 Rodil, R., Quintana, J.B. and Cela, R. (2012) Transformation of phenazone-type drugs
568 during chlorination. Water Research 46(7), 2457–2468.

569 Schulze, S., Zahn, D., Montes, R., Rodil, R., Quintana, J.B., Knepper, T.P., Reemtsma, T.
570 and Berger, U. (2019) Occurrence of emerging persistent and mobile organic
571 contaminants in European water samples. Water Research 153, 80-90.

572 Tang, J., Tang, L., Zhang, C., Zeng, G., Deng, Y., Dong, H., Wang, J. and Wu, Y. (2015)
573 Different senescent HDPE pipe-risk: brief field investigation from source water to tap
574 water in China (Changsha City). Environmental Science and Pollution Research 22(20),
575 16210-16214.

576 Tawk, A., Deborde, M., Labanowski, J. and Gallard, H. (2015) Chlorination of the β -
577 triketone herbicides tembotrione and sulcotrione: Kinetic and mechanistic study,
578 transformation products identification and toxicity. Water Research 76, 132-142.

579 Zahn, D., Mucha, P., Zilles, V., Touffet, A., Gallard, H., Knepper, T.P. and Frömel, T.
580 (2019) Identification of potentially mobile and persistent transformation products of
581 REACH-registered chemicals and their occurrence in surface waters. Water Research
582 150, 86-96.

583

584

585 **LIST OF TABLES**

586 Table 1. QSAR Predicted toxicity values for DPG and its TPs.

587 Table 2. QSAR Predicted toxicity values for DTG and its TPs.

588

589 **LIST OF FIGURES**

590 Figure 1. pH dependence of the experimental and modelled apparent rate constants of
591 chlorination of (a) DPG and (b) DTG.

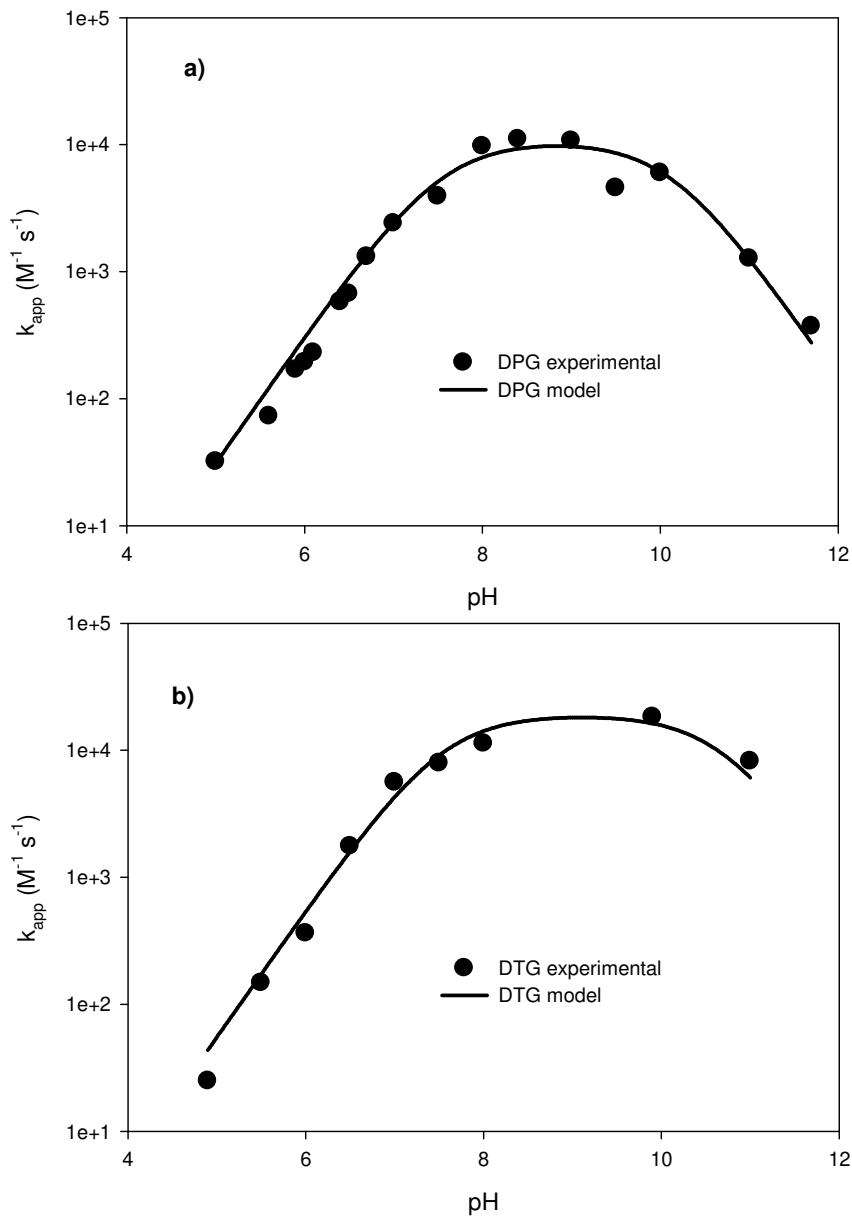
592 Figure 2. pH dependence of the experimental (symbols) and modelled apparent rate
593 constants of bromination of (a) DPG and (b) DTG. Direct kinetic method (circle) and
594 competitive kinetic method using 4-bromophenol (square) or 2,4,6-tribromophenol
595 (triangle) as reference compounds were used for k_{app} determination. Only full symbols
596 were used for model calculation.

597 Figure 3. Schematic representation of DPG TPs

598 Figure 4. Schematic representation of DTG TPs.

599 Figure 5. Evolution of bioluminescence inhibition measured using *Vibrio fischeri*
600 Microtox® test during DPG chlorination. $[DPG]_0 = 40 \text{ mg Cl}_2 \text{ L}^{-1}$, molar DPG:Cl₂ ratios of
601 1:3 and 1:30, chlorination time of 4 days at pH 7.0.

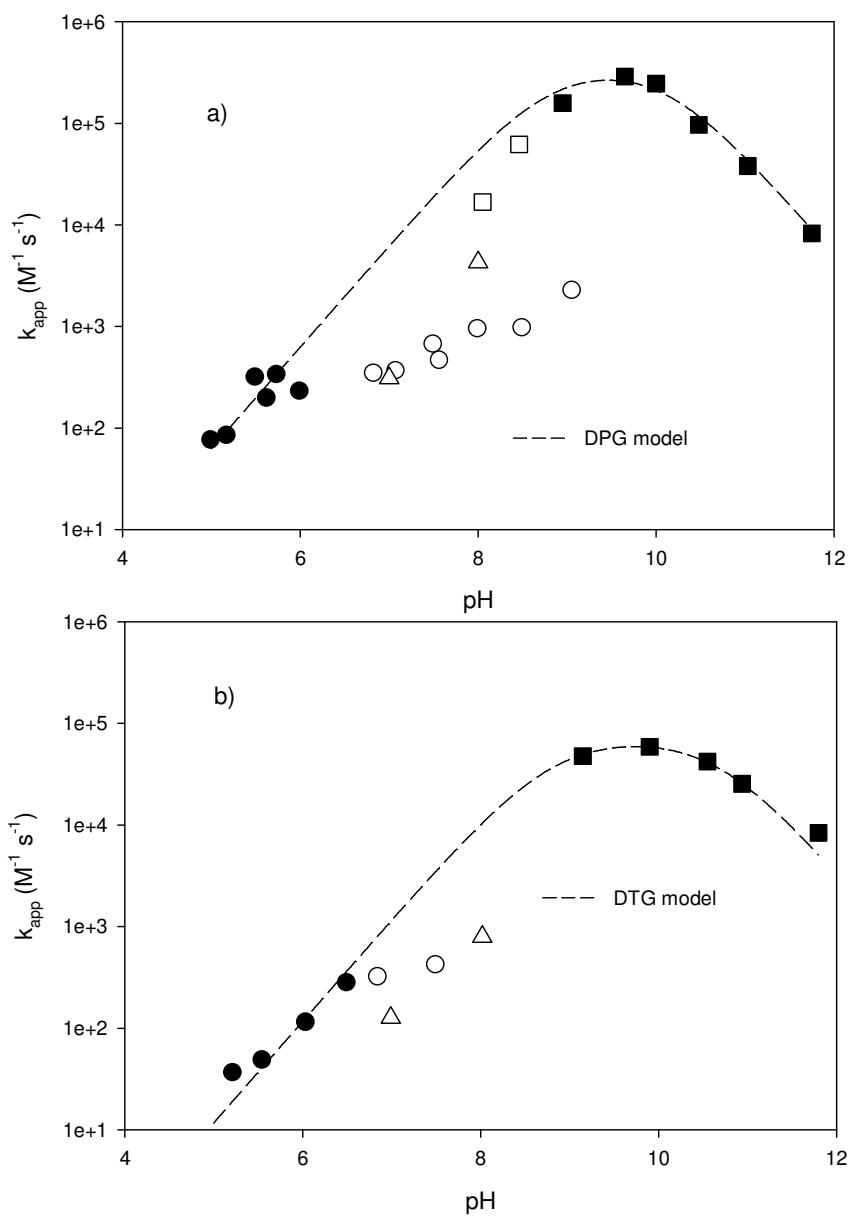
602



603

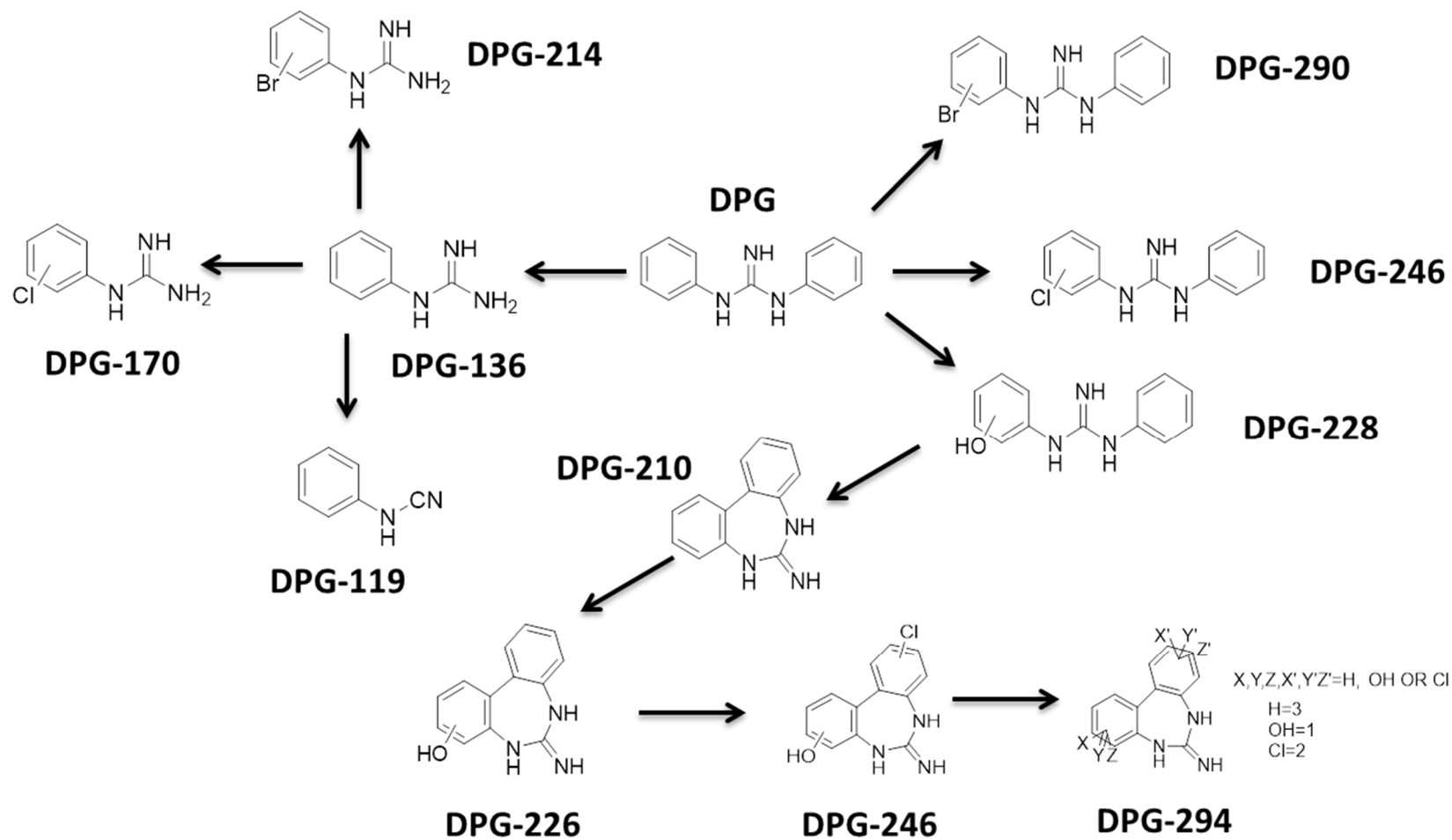
604 Figure 1. pH dependence of the experimental and modelled apparent rate constants of

605 chlorination of (a) DPG and (b) DTG.



606

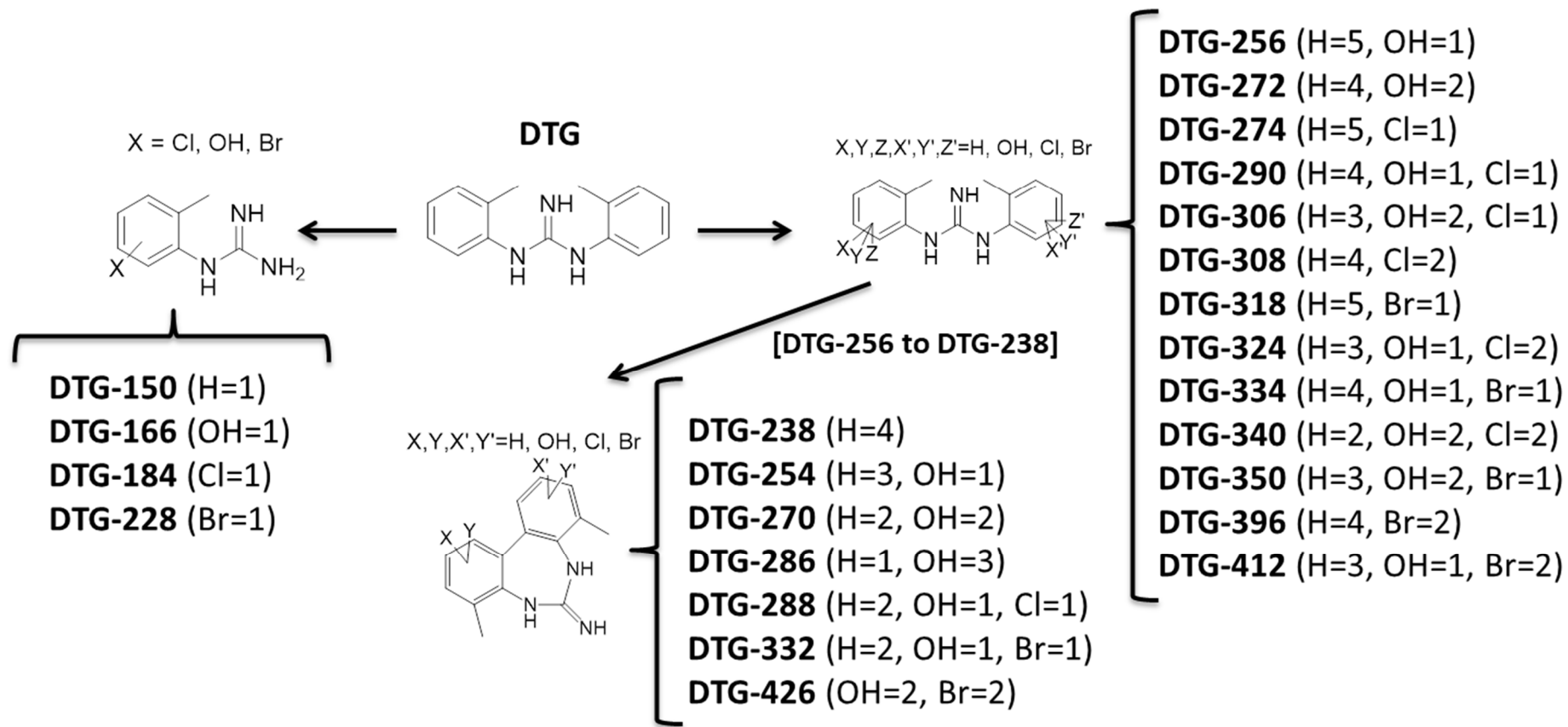
607 Figure 2. pH dependence of the experimental (symbols) and modelled apparent rate
 608 constants of bromination of (a) DPG and (b) DTG. Direct kinetic method (circle) and
 609 competitive kinetic method using 4-bromophenol (square) or 2,4,6-tribromophenol
 610 (triangle) as reference compounds were used for k_{app} determination. Only full symbols
 611 were used for model calculation.



612

613 Figure 3. Schematic representation of DPG TPs

614

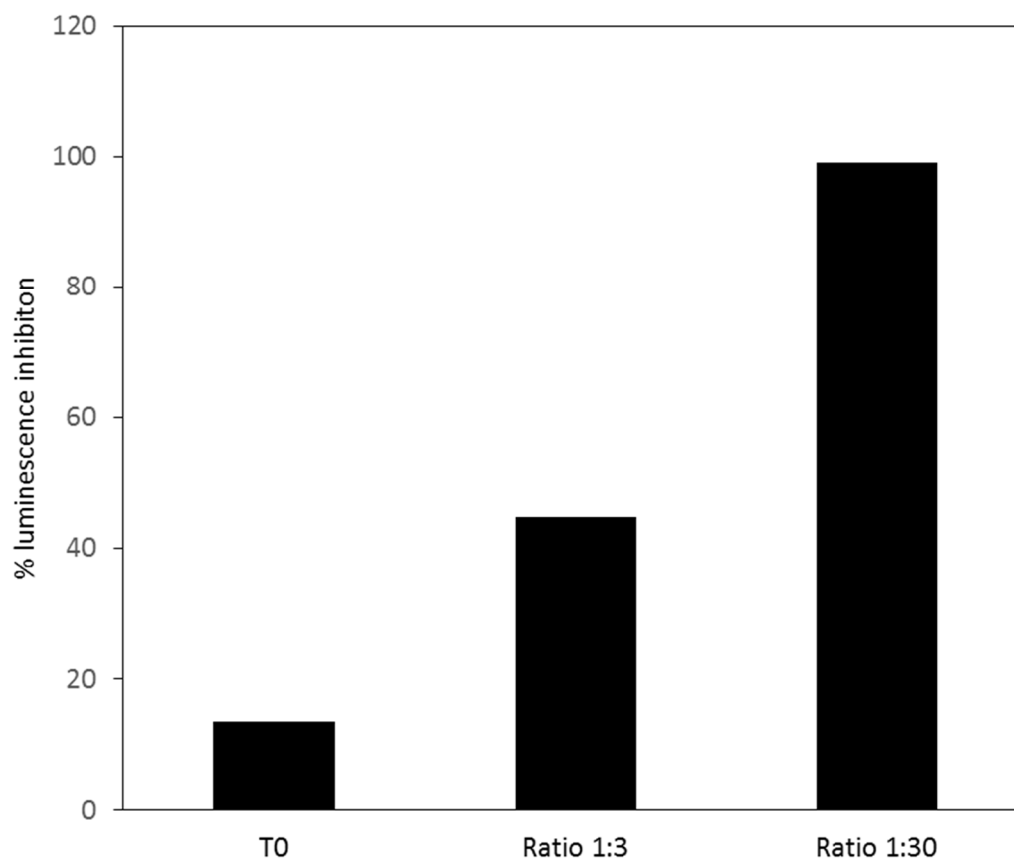


615

616 Figure 4. Schematic representation of DTG TPs

617

618



620

621 Figure 5. Evolution of bioluminescence inhibition measured using *Vibrio fischeri*
622 Microtox® test during DPG chlorination. $[DPG]_0 = 40 \text{ mg Cl}_2 \text{ L}^{-1}$, molar DPG:Cl₂ ratios of
623 1:3 and 1:30, chlorination time of 4 days at pH 7.0.

624

625

Table 1. QSAR Predicted toxicity values for DPG and its TPs.

	<i>Daphnia magna</i>	<i>T. pyriformis</i>	Oral rat
	LC ₅₀ (48 hr) (mg/L)	IGC ₅₀ (48 hr) (mg/L)	LD ₅₀ (mg/kg)
DPG	5.09	28.5	805
DPG-119	16.4	np	493
DPG-136	30.6	np	500
DPG-170	11.5	np	455
DPG-210	5.29	11.4	908
DPG-214	1.14	9.53	1320
DPG-226	2.46	10.4	1143
DPG-228	5.24	21.1	2433
DPG-246	1.22	7.21	886
DPG-260	1.89	4.78	1241
DPG-290	1.14	9.53	1320
DPG-294	0.75	2.88	1019

np: no prediction possible

Table 2. QSAR Predicted toxicity values for DTG and its TPs.

	<i>Daphnia magna</i>	<i>T. pyriformis</i>	Oral rat
	LC ₅₀ (48 hr) (mg/L)	IGC ₅₀ (48 hr) (mg/L)	LD ₅₀ (mg/kg)
DTG	2.92	5.53	602
DTG-150	27.5	np	498
DTG-166	23.5	np	993
DTG-184	22.7	np	429
DTG-228	5.00	np	519
DTG-238	3.14	6.35	553
DTG-254	1.68	8.26	1036
DTG-256	3.43	9.19	1259
DTG-270	2.16	6.52	1121
DTG-272	2.52	11.2	2352
DTG-274	0.70	2.29	1178
DTG-286	8.28	9.80	527
DTG-288	0.76	1.98	721
DTG-290	0.93	2.14	1014
DTG-306	0.95	2.06	1870
DTG-308	0.49	1.24	1109
DTG-318	0.39	4.35	1103
DTG-324	0.74	1.11	940
DTG-332	0.51	1.55	1627
DTG-334	0.87	3.21	927
DTG-340	0.31	1.11	1074
DTG-250	0.79	2.38	1485
DTG-396	0.19	1.46	563
DTG-412	0.28	1.21	823
DTG-426	0.03	0.55	384

np: no prediction possible

